

# Heat extraction from a salinity-gradient solar pond using in pond heat exchanger

M.R. Jaefarzadeh \*

*Civil Engineering Department, Ferdowsi University of Mashhad, P.O. Box 91775-1111 Mashhad, Iran*

Received 10 September 2005; accepted 28 January 2006

Available online 10 March 2006

## Abstract

Thermal energy extraction from a small salinity-gradient solar pond is studied in this article. The small pond has an area of 4.0 m<sup>2</sup> and a depth of 1.1 m. Fresh water circulates through an internal heat exchanger, located in the lower convective zone, and transfers its thermal energy to an external heat exchanger. The study covers two periods of summer loading for a week and winter loading for two months. The hourly as well as daily variations of the temperatures of the storage zone, surface zone, ambient, inlet and outlet of the internal heat exchanger have been measured and analyzed. It is shown that the pond may deliver heat with a relatively high thermal efficiency in a transitional stage for a limited period of time. It can also be utilized continuously with a lower efficiency. The efficiency of the small pond in the latter case will be around 10%.

© 2006 Elsevier Ltd. All rights reserved.

*Keywords:* Heat extraction; Salinity-gradient solar pond

## 1. Introduction

Energy extraction for domestic and industrial heating purposes, or for converting to refrigeration or electricity, is the ultimate aim in the design and construction of a solar pond. There are two common methods for energy removal from a solar pond.

In the first method, hot saline water is pumped out through a diffuser, and after extracting some of its thermal energy, returned back to the pond by another diffuser. The first diffuser is located in the storage zone, close to the lower interface, and the second diffuser is installed near to the bottom of the pond. The fluid velocity, at the diffuser level, is regulated to prevent the erosion of the gradient layer. This method was applied in many countries, such as Israel in the Dead Sea [1], India in Bhuj [2], and USA, at the University of New Mexico [3], and the University of Texas at El Paso [4].

In the second method hot water circulates, in a closed cycle, through a series of pipes installed in the pond as internal heat exchanger (IHE), and transfers its thermal energy to an external heat exchanger (EHE). The best position for the IHE is in the storage zone near to the gradient layer. Thereby, heat extraction stimulates the convection process in the thickness of the lower convective zone (LCZ). The IHE may be made from metallic or plastic pipes. In the metallic pipe system, the maximum rate of heat extraction is controlled by the natural convection intensity; whereas in the plastic pipe system the thermal conductivity of the pipe material will restrain the amount of heat removal. Therefore, a larger pipe area is needed for this case [5]. The final decision may be approached by an accurate cost analysis.

The IHE may be installed on a frame that is fixed at the bottom of the pond, or suspended from an external structure. This method was applied for the energy removal from a 200 m<sup>2</sup> pond at the Ohio State University [6], and recently from a 3000 m<sup>2</sup> pond at Pyramid Hill in Australia [7].

An experimental salinity-gradient solar pond with an area of 4 m<sup>2</sup> and a depth of 1.1 m was built at Ferdowsi

\* Fax: +98 511 8436 433.

E-mail address: [jafarzad@ferdowsi.um.ac.ir](mailto:jafarzad@ferdowsi.um.ac.ir)

### Nomenclature

$A$	external area of the pipe ( $\text{m}^2$ )	$\Delta T$	temperature difference ( $^\circ\text{C}$ )
$C$	specific heat ( $\text{J kg}^{-1} \text{ }^\circ\text{C}^{-1}$ )	$\xi$	ratio of daily heat extraction to daily irradiation received by the pond surfaces (%)
$D$	thermal diffusivity ( $\text{m}^2 \text{ s}^{-1}$ )	$\nu$	kinematic viscosity ( $\text{m}^2 \text{ s}^{-1}$ )
$d$	pipe diameter (m)		
EHE	external heat exchanger		
$g$	acceleration of gravity ( $\text{m s}^{-2}$ )	<i>Dimensionless numbers</i>	
$h$	convective heat transfer coefficient ( $\text{W m}^{-2} \text{ }^\circ\text{C}^{-1}$ )	$Nu$	Nusslet number
IHE	internal heat exchanger	$Ra$	Rayleigh number
$k$	thermal conductivity ( $\text{W m}^{-1} \text{ }^\circ\text{C}^{-1}$ )	$Gr$	Grashof number
LCZ	lower convective zone of the solar pond	$Pr$	Prandtl number
$\dot{m}$	mass flow rate ( $\text{kg s}^{-1}$ )		
NCZ	non-convective zone of the solar pond	<i>Subscripts</i>	
$Q$	rate of heat extraction (W)	i	internal, inlet
$T$	temperature ( $^\circ\text{C}$ )	e	external
$U$	overall heat transfer coefficient ( $\text{W m}^{-2} \text{ }^\circ\text{C}^{-1}$ )	o	outlet
UCZ	upper convective zone of the solar pond	p	pipe, pond
$\beta$	thermal expansion coefficient ( $^\circ\text{C}^{-1}$ )	m	mean

University of Mashhad in the north east of Iran ( $36^\circ16'\text{N}$ ,  $59^\circ37'\text{E}$ ). The performance of the pond has been monitored for several years and reported in a series of publications [8–10]. A system of internal heat exchanger was designed for energy removal from the pond. In this paper, we describe the system and present our experiences for two periods of heat extraction in the winter of 1998–1999 and summer of 2000. Thereby, the overall efficiency of the pond will be estimated.

## 2. Description of the heat removal system

A schematic view of the heat extraction system is shown in Fig. 1. The system is composed of the following elements:

1. An IHE made from a polyethylene pipe, with an internal diameter of 16 mm, an external diameter of 20 mm, and a length of 14.4 m. This pipe is fixed on a frame 30 cm above the bottom of the pond in the LCZ.
2. An air chamber consists of a double sided plastic cylinder. Fine bubbles of air may be released from the circulating fluid (water) in this container. It is also possible to regulate the volume of the circulated water by the container.
3. A variable speed pump for the circulation of water.
4. An EHE, similar to a car radiator, with copper pipes that are cooled down by the blow of air from a variable speed fan.
5. An orifice meter.
6. Four thermal sensors (PT100) installed at the inlet and outlet pipes of the IHE and EHE.
7. A valve for controlling the amount of discharge.

## 3. In-pond heat exchanger performance

The rate of heat extraction from the solar pond is given by

$$Q = AU \frac{(T_o - T_i)}{\ln \frac{T_p - T_i}{T_p - T_o}} \quad (1)$$

where  $A$  is the external area of the pipe,  $U$  is the overall coefficient of heat transfer,  $T_p$ ,  $T_o$  and  $T_i$  are the temperatures of the pond, outlet and inlet to the in-pond heat exchanger (IHE), respectively.

The consumed energy, at the EHE, and the piping system out of the pond, is obtained from

$$Q = \dot{m} C (T_o - T_i), \quad (2)$$

where  $\dot{m}$  is the mass flow rate, and  $C$  is the specific heat of the circulating water.

The outlet temperature can be calculated from Eqs. (1) and (2) as

$$T_o = T_p - \frac{(T_p - T_i)}{\exp\left(\frac{UA}{\dot{m}C}\right)}. \quad (3)$$

In Eq. (3), the inlet temperature depends on the consumed energy out of the solar pond, the pond temperature depends on the absorbed energy at the storage zone (LCZ), and the exponential term  $\frac{UA}{\dot{m}C}$  is a function of the geometrical and thermo-physical characteristics of the IHE, circulating fluid, and its discharge. By increasing the overall coefficient of heat transfer, or the area of the IHE, the value of  $T_o$ , or the amount of extracted energy from the pond will

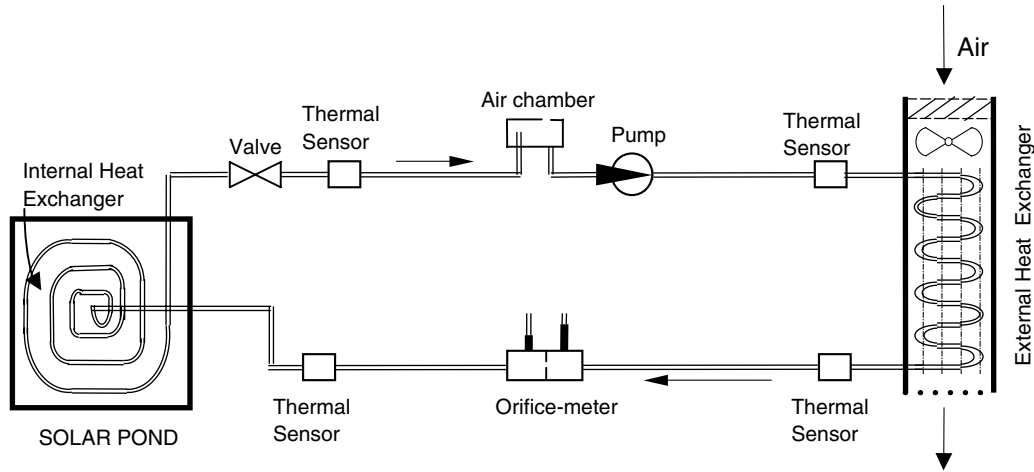


Fig. 1. Schematic view of the solar pond and the system of heat extraction.

increase, while by enhancing the discharge or the specific heat of the fluid the outlet temperature will decrease.

The overall coefficient of heat transfer  $U$  is given by

$$U = \frac{1}{\frac{d_e}{d_i} \frac{1}{h_i} + \frac{d_e}{2k_p} \ln \left( \frac{d_e}{d_i} \right) + \frac{1}{h_e}}, \quad (4)$$

where  $h_e$  and  $h_i$  are the convective coefficients of the heat transfer of the fluids inside and outside of the IHE,  $k_p$  is the conductive coefficient of the heat transfer of the pipe material, and  $d_e$  and  $d_i$  are the internal and external diameters of the pipe [11]. In the denominator of Eq. (4), the first and last terms represent the thermal resistances due to the convective boundaries at the inside and outside of the pipe, and the middle term represents the conductive resistance of the pipe material.

In our experiments, the fluid velocity in the pipe was so small, in the order of a few centimeters per second, so that the Reynolds number was usually in the laminar flow range. Therefore, the Nusselt number was constant for the forced convective heat transfer [12]

$$Nu_i = \frac{h_i d_i}{k_i} = 3.66, \quad (5)$$

where  $k_i$  is the coefficient of conductive heat transfer of the circulating fluid.

The average Nusselt number  $Nu_m$ , for a free convective flow with a uniform temperature, around a cylindrical pipe, is given by

$$Nu_m = \frac{h_e d_e}{k_e} = c Ra^n \quad 10^{-10} \leq Ra \leq 10^{12}, \quad (6)$$

where  $k_e$  is the conductive coefficient of heat transfer of the surrounding fluid (saline),  $Ra$  is the dimensionless Rayleigh number,  $c$  and  $n$  are constant coefficients defined in Table 1 [12].

Rayleigh number is defined by

$$Ra = \frac{g \beta \Delta T d_e^3}{\nu D}, \quad (7)$$

Table 1  
Variation of  $c$  and  $n$  versus  $Ra$

$Ra$	$c$	$n$
$10^{-10}$ – $10^{-2}$	0.675	0.058
$10^{-2}$ – $10^2$	1.02	0.148
$10^2$ – $10^4$	0.85	0.188
$10^4$ – $10^7$	0.48	0.25
$10^7$ – $10^{12}$	0.125	0.333

where  $g$  is the acceleration due to gravity,  $\beta$  is the coefficient of thermal expansion,  $\Delta T$  is the temperature difference of the pipe and the ambient fluid,  $\nu$  is the coefficient of kinematic viscosity, and  $D$  is the thermal diffusivity.

#### 4. Experimental studies on heat removal from the solar pond

Two series of experiments in the summer of 2000 and winter of 1998–1999 were conducted in the solar pond. We explain the results for each series separately.

##### 4.1. Heat removal in the summer

Heat removal from the pond was performed from 30 May to 6 June 2000. The pump discharge was  $16.82 \text{ cm}^3/\text{s}$ . In Fig. 2, the daily average temperatures of the LCZ and the ambient have been plotted from 25 May to 23 June for about a month. In the same figure the inlet and outlet temperatures of the heat exchanger to the pond have been plotted during the loading period. As seen, before the heat removal the LCZ temperature had been fixed at about  $59^\circ\text{C}$ . In the first four days, i.e. the transitional stage, it reduced to about  $40^\circ\text{C}$ , and then, for the next four days, i.e. the quasi-steady stage, it remained nearly constant. After the loading period, the LCZ temperature rose quickly to  $50^\circ\text{C}$  in the first week and then to about  $58^\circ\text{C}$  in the next two weeks. The ambient temperature was changing all through the month. However, its effect on the LCZ temperature was insignificant.

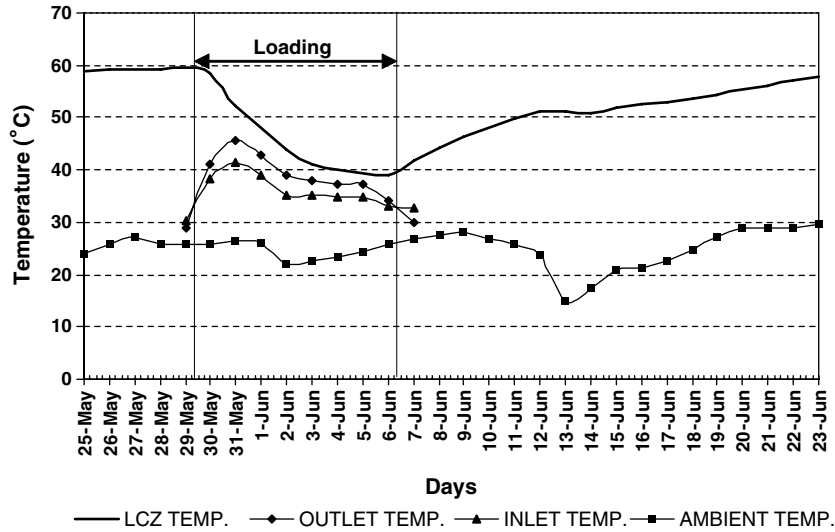


Fig. 2. Daily average temperatures of the LCZ, ambient, inlet and outlet to heat exchanger.

Fine examination of the outlet temperature reveals that when the heat extraction began the outlet temperature rose to a maximum of 47 °C in two days. It dropped to 38 °C in the next two days, and then became stable for the last three days. Inlet temperature had a similar trend as the outlet temperature.

In Fig. 3, the hourly average temperatures of the UCZ and LCZ have been drawn for 480 h from 25 May to 15 June. The observed sinusoidal variation of the temperature during each day is a function of the varying intensity of the solar radiation. There is also a phase lag between the UCZ and LCZ curves, and the daily fluctuation of the temperature in the UCZ is much higher than the LCZ. Heat removal has considerably reduced the temperature of the LCZ. However, its effect on the variation of the UCZ temperature is insignificant.

In Fig. 4, variation of the temperature profiles in the depth of the pond at different hours in several days has been plotted for 29 May (one day before loading), 2 June, 5 June and 10 June (a few days after the loading period). As

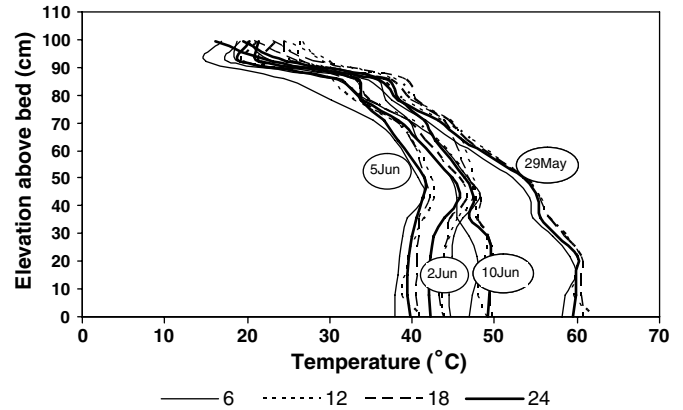


Fig. 4. Temperature profiles in depth of solar pond at different hours in several days.

seen, the UCZ and LCZ thicknesses are 15 and 40 cm, respectively, leaving an NCZ of about 50 cm. The dramatic change in the temperature of the LCZ may also be deduced from this figure. However, the heat removal effect has been diminished on the upper half depth of the pond. A similar trend has also been reported by Hull et al. in their 1000 m<sup>2</sup>–4 m depth solar pond in the Argonne National Laboratory [13].

Fig. 5 depicts a detailed history of the loading process, showing the hourly variation of the LCZ, outlet, inlet, and ambient temperatures, during the heat removal period. In the transitional stage (0–96 h), there was a significant difference between the outlet and inlet temperatures, all through the days. In the quasi-steady stage (96–192 h), the LCZ, inlet and outlet temperatures came close during the days, implying a negligible heat removal, and went far from each other and from the ambient temperature at nights, when the heat removal was considerable.

Fig. 6 shows the hourly fluxes of solar radiation and energy extraction from the pond during the loading period.

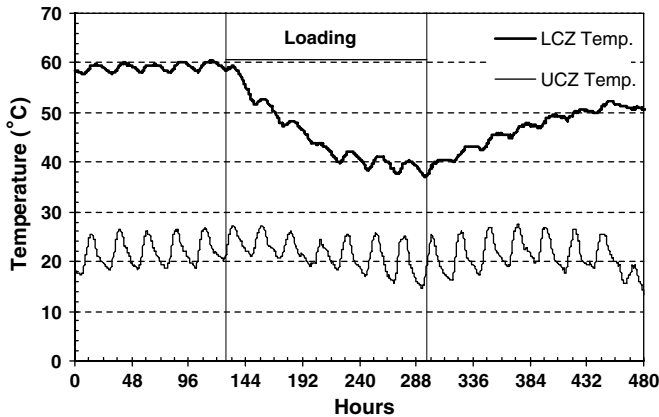


Fig. 3. Hourly temperatures of the LCZ and UCZ, 25 May–15 June.

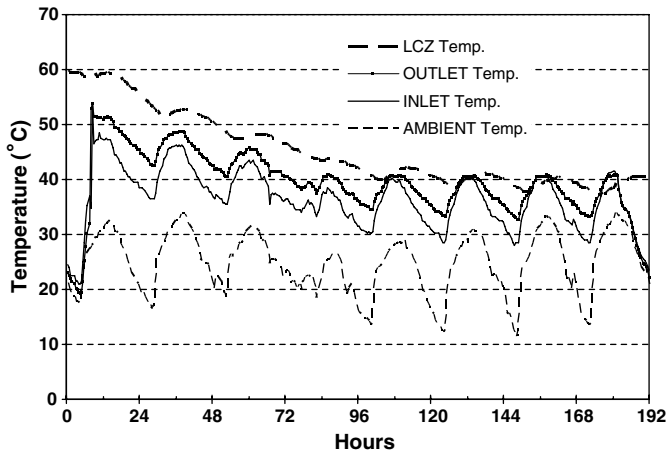


Fig. 5. Hourly temperatures of the LCZ, ambient, inlet and outlet to heat exchanger during the loading period.

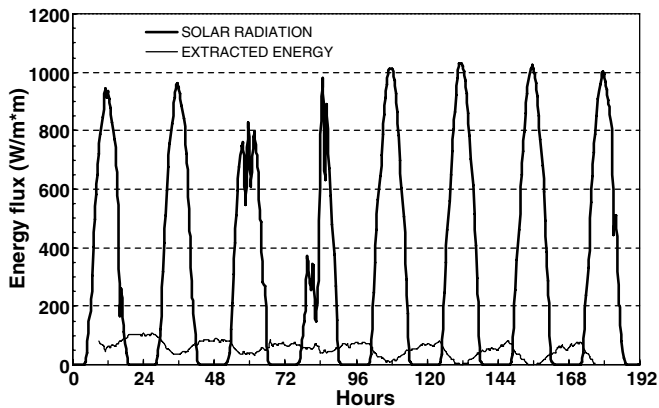


Fig. 6. Hourly fluxes of solar radiation and energy extraction from the pond.

As seen, in the transitional stage, heat was extracted, continuously, 24 h per day. However, in the quasi-steady state heat could only be removed at nights.

In Fig. 7, the daily average fluxes of solar irradiation and extracted energy together with lost energies through the sides, bottom and NCZ have been plotted. The lost energy fluxes were calculated by differentiating the temperatures of the in-pond sensors and the sensors that were mounted at certain points in the insulating sheets surrounding the sides and bottom of the pond. Because of thick polystyrene sheets, the lost energy fluxes through the bottom and sides were negligible. However, for the slightly thin NCZ, the upward lost energy was considerable. Notwithstanding, the biggest share of the total energy removal was allocated to heat extraction. Daily irradiation flux was fairly uniform in the first three days and the last four days. However, it had a minimum value on the 2 June.

The parameter  $\xi$  is defined as the ratio of the daily used heat to the total daily irradiation energy received by the pond surface. In Fig. 8, the values of  $\xi$  are plotted for 8 days during the summer loading period. It may be seen that in the transient stage  $\xi$  is about 21%, though reduction in

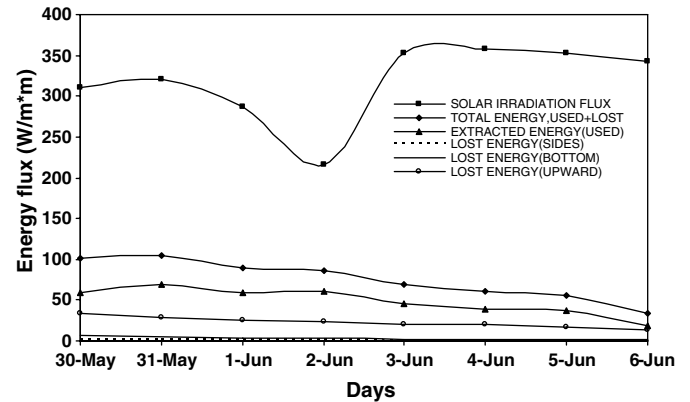


Fig. 7. Daily average fluxes of solar radiation, energy extraction and lost energies.

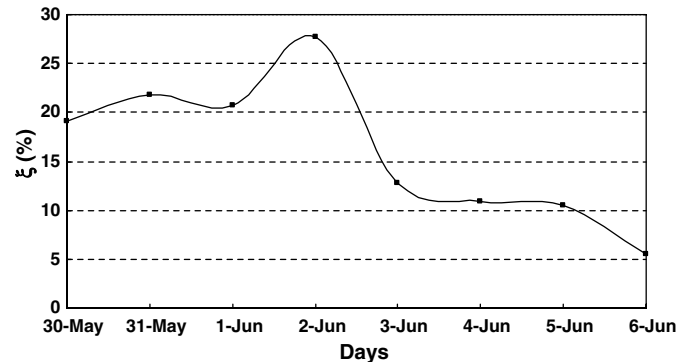


Fig. 8. The ratio of used heat to received solar irradiation in summer loading.

solar energy and ambient temperature temporarily raised  $\xi$  to 27% on the 2 June. In the following three days, however, when the LCZ heat storage is exhausted,  $\xi$  approached its steady state value of 11%. This value may be taken as the efficiency of the small pond. The loading process was ceased in the middle of the last day.

#### 4.2. Heat removal in the winter

In the winter of 1998–1999 the loading period started on 6 November and took for two months. The pump discharge was  $13 \text{ cm}^3/\text{s}$ . Fig. 9 shows the daily average temperatures of the LCZ, ambient, inlet and outlet to the pond from 1 November to 31 January. It may be noted that the temperature of the LCZ, being  $36^\circ\text{C}$  at the start of the loading period, dropped to  $7^\circ\text{C}$  when the heat extraction ceased on the 6 January. Thereafter, the LCZ temperature increased steadily and independently from the fluctuations of the ambient temperature. In Fig. 10, the hourly variation temperatures of the LCZ and UCZ have been drawn for 552 h from 1 to 23 November. All of the records were complete and accurate in this period. It is clearly shown that the LCZ temperature that was uniform and around  $36^\circ\text{C}$  before the loading reduced to  $20^\circ\text{C}$  in eight days (6–19

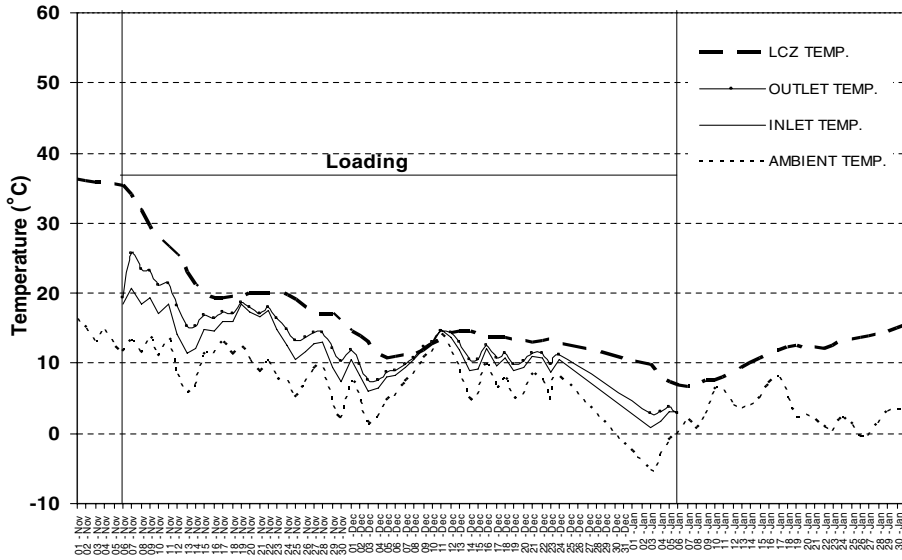


Fig. 9. Daily average temperatures of the LCZ, ambient, inlet and outlet to the heat exchanger in winter.

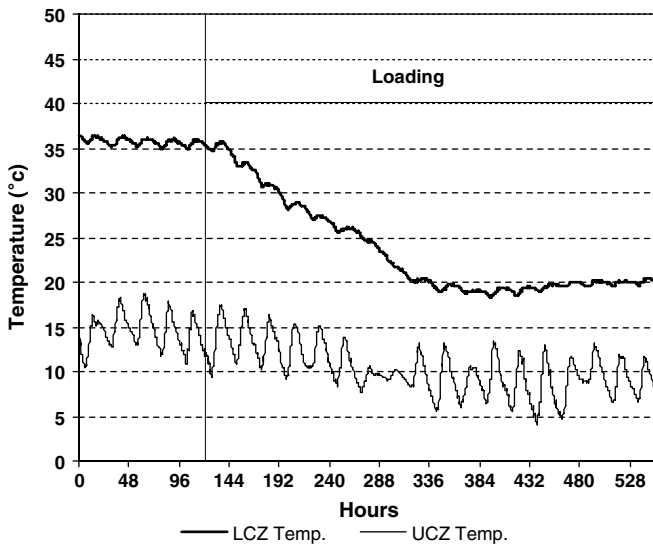


Fig. 10. Hourly temperatures of the LCZ and UCZ in November 1998.

November). This happened at the transient stage when the maximum energy was extracted from the pond. Then, the LCZ temperature remained quasi-steady in the remaining few days.

In Fig. 11, the daily average radiation influx and used heat flux have been plotted from 1st to 23 November. It may be seen that the radiation intensity was low and fluctuating. In the transient stage, heat extraction though variable, was well above 50 W/m<sup>2</sup> and even from 11 to 14 November the amount of energy withdrawal was more than the solar irradiation received by the pond surface. However, in the following days the energy extraction rate declined steadily and reached a minimum of 10 W/m<sup>2</sup>.

Fig. 12 depicts  $\zeta$  that is the ratio of the daily used heat to the daily received solar irradiation. It may be seen that the average value of  $\zeta$  in the transient stage was about 50% of

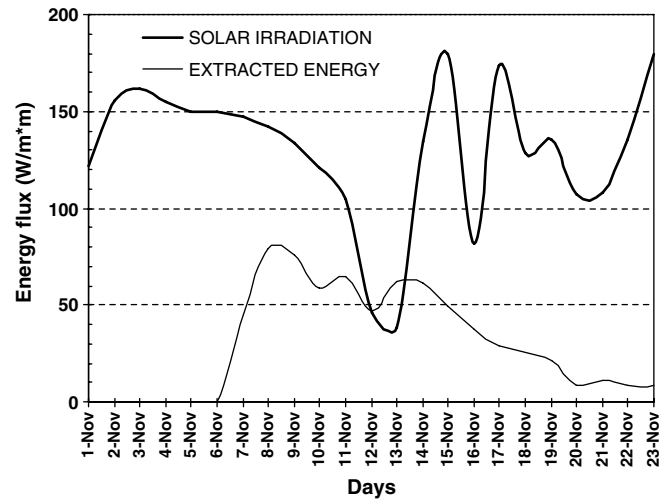


Fig. 11. Daily average radiation influx and used heat flux.

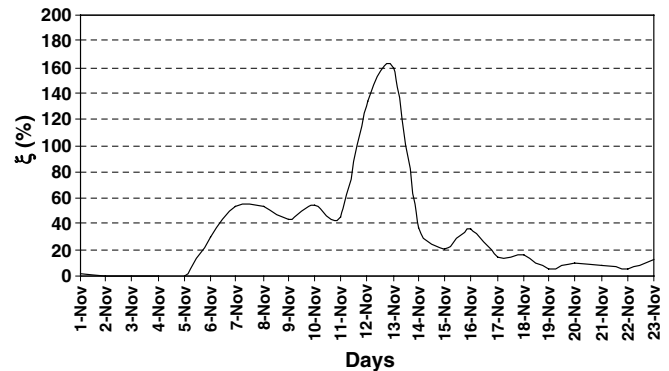


Fig. 12. The ratio of used heat to received solar irradiation in November 1998.

the influx. The singular peak of the curve that occurred in 11–14 November corresponded to the cloudy days that



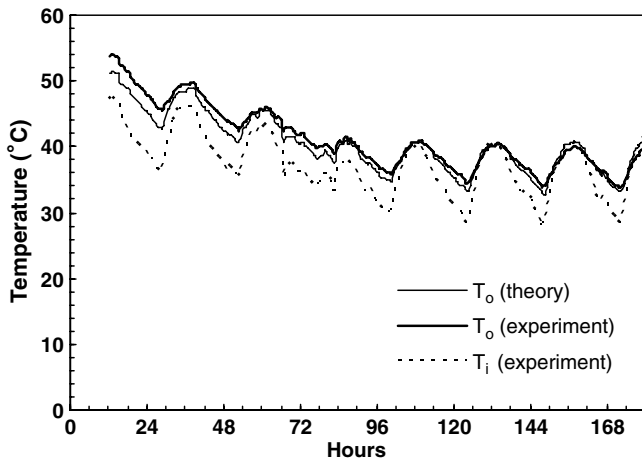


Fig. 13. Hourly average theoretical and experimental values of the outlet temperature of heat exchanger in summer loading.

irradiation intensity was low and should not be misinterpreted as a remarkable energy removal rate. The average value of the quasi-steady heat removal, from 19 to 23 November, was about 10% of the daily irradiation. The average value of  $\xi$  in this stage was close to that in summer period implying a pond efficiency of about 10% in the steady state situation.

#### 4.3. Verification of the theoretical model

Substituting for the thermo-physical parameters available from the standard handbooks in Eq. (4), we will obtain a theoretical value for the overall coefficient of heat transfer  $U = 56 \text{ W/m}^2$  for the summer loading. This value corresponds to a total thermal resistance of  $R = 0.0179$ , where 55% of it is attributed to the inside convective resistance, 30% to the conductive resistance of the pipe material

and 15% to the outer free convective resistance. The overall coefficient of heat transfer for the winter loading is  $U = 50 \text{ W/m}^2$ . The theoretical outlet temperature may be obtained from Eq. (3) by substituting for the pond (LCZ) temperature, inlet temperature, and the geometrical and thermo-physical characteristics of the IHE. Fig. 13 shows the theoretical  $T_o$  together with the hourly measured values of  $T_i$  and  $T_o$  for the summer loading period. The agreement between the theory and experiment is quite satisfactory. Fig. 14 shows the daily average values of the theoretical  $T_o$  together with the daily average measured values of  $T_i$  and  $T_o$  for the winter loading. The conformity in the winter loading is less than the summer loading. This may be attributed to an overestimation of the theoretical value of  $U$  in the winter.

## 5. Conclusions

The performance of a small-scale solar pond in two periods of summer and winter energy extraction has been studied in this article. A polyethylene pipe, used as an internal heat exchanger, was located at the storage zone. Fresh water circulated in a closed loop transferred the thermal energy of the storage zone to an air to water external heat exchanger.

The rate of decrease in the temperature of the LCZ was very high in a transitional period of heat extraction. However, the LCZ temperature became uniform gradually, and reduced to a quasi-steady state situation.

Therefore, a solar pond may serve as an emergency source of energy for a peak load in a short period of time. It may also be used continuously as an energy reserve. The efficiency of the small pond was about 10% in steady state condition. Based on our calculations for a large-scale solar pond we may have an increase in efficiency up to 22% in this geographical latitude [14].

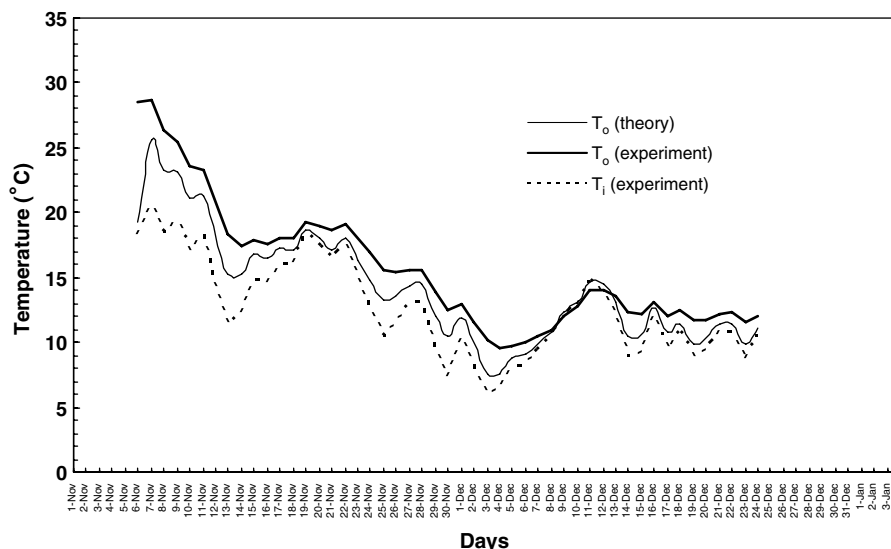


Fig. 14. Daily average theoretical and experimental values of the outlet temperature of heat exchanger in winter loading.

The performance of the in-pond heat exchanger may be evaluated by estimating a value for the overall coefficient of heat transfer. The theoretical values for the outlet temperature were in good agreement with the experimental measurements in the summer loading period. In winter loading, the values were fairly good due to a possible over-estimation in the values of the overall coefficient of heat transfer.

### Acknowledgements

The support of the research council of Ferdowsi University of Mashhad during the preparation of this work is kindly acknowledged. The author would like to appreciate the efforts of the late Mr. Khaleghzadeh for setting up the experimental apparatus.

### References

- [1] H.Z. Tabor, B. Doron, The Beith Ha' Arava 5 MW(e) solar pond power plant (SPPP)—progress report, *Solar Energy* 45 (4) (1990) 247–253.
- [2] V.V.N. Kishore, A. Kumar, Solar pond: an exercise in development of indigenous technology at Kutch, India, *Energy Sustain Dev* 3 (1) (1996) 17–28. Available from: <<http://www.teriin.org/division/eetdiv/docsft01.ht>>.
- [3] F. Zangrando, H.C. Bryant, Heat extraction from a salt gradient solar pond, in: International Conference on Alternative Energy Sources, Miami Beach, FL, 1977, also in *Solar Age*, 1978, April.
- [4] A. Swift, Salinity Gradient Solar Ponds, Practical Manual. Part II: solar pond operation and maintenance, The El Paso Solar Pond Project, 1995.
- [5] J. Hull, C.E. Nielsen, P. Golding, Salinity Gradient Solar Ponds, CRC Press, Boca Raton, FL, 1989.
- [6] C.E. Nielsen, Non-convective salt gradient solar ponds, in: W.C. Dickinson, P.N. Cheremisinoff (Eds.), *Solar Energy Technology Handbook*, Marcel Dekker, New York, 1980, pp. 345–376 (Chapter 11).
- [7] A. Akbarzadeh, J. Andrews, P. Golding, Integration of solar ponds in salinity mitigation schemes to produce low grade heat for industrial process heating, desalination and power, in: Proceedings of 2005 Solar World Congress Bringing Water to the World, Orlando, FL, August 8–12, 2005, pp. 233–294.
- [8] M.R. Jaefarzadeh, Thermal behavior of a small salinity-gradient solar pond with wall shading effect, *Solar Energy* 77 (2004) 281–290.
- [9] M.R. Jaefarzadeh, Evaluation of the methods for gradient establishment in salinity gradient solar ponds, *Int. J. Eng.* 14 (3) (2003) 149–159.
- [10] M.R. Jaefarzadeh, On the performance of a salinity-gradient solar pond, *Appl. Therm. Eng.* 20 (2000) 243–252.
- [11] F. Sabetta, M. Pacetti, P. Principi, An internal heat extraction system for solar ponds, *Solar Energy* 34 (4/5) (1985) 297–302.
- [12] M.N. Özışık, *Heat Transfer A Basic Approach*, third ed., McGraw-Hill, 1988.
- [13] J.R. Hull, A.B. Scranton, J.M. Mehta, S.H. Cho, K.E. Kasza, Heat extraction from the ANL research salt gradient solar pond, Report ANL-86-17, Argonne National Laboratory, Argonne, IL, 1986.
- [14] M.R. Jaefarzadeh, Thermal behavior of a large salinity-gradient solar pond in the city of Mashhad, Iran. *J. Sci. Technol.* 29 (B2) (2005) 219–229.